POWQMIX:
Weighted Value Factorization with Potentially Optimal Joint Actions Recognition for Cooperative Multi-Agent Reinforcement Learning

Chang Huang[*1], **Shatong Zhu**[*1], **Junqiao Zhao**[1†],
Hongtu Zhou[1], **Chen Ye**[1], **Tiantian Feng**[1], **Changjun Jiang**[1]

[1]Tongji University

Abstract

Value function factorization methods are commonly used in cooperative multi-agent reinforcement learning, with QMIX receiving significant attention. Many QMIX-based methods introduce monotonicity constraints between the joint action value and individual action values to achieve decentralized execution. However, such constraints limit the representation capacity of value factorization, restricting the joint action values it can represent and hindering the learning of the optimal policy. To address this challenge, we propose the **P**otentially **O**ptimal Joint Actions **W**eighted QMIX (POWQMIX) algorithm, which recognizes the potentially optimal joint actions and assigns higher weights to the corresponding losses of these joint actions during training. We theoretically prove that with such a weighted training approach the optimal policy is guaranteed to be recovered. Experiments in matrix games, difficulty-enhanced predator-prey, and StarCraft II Multi-Agent Challenge environments demonstrate that our algorithm outperforms the state-of-the-art value-based multi-agent reinforcement learning methods.

1 Introduction

Multi-agent reinforcement learning (MARL) is promising to solve cooperative tasks in many fields, including robot swarms (Huang et al. 2020), autonomous driving, (Schmidt et al. 2022) and gaming (Terry et al. 2021). However, simultaneous policy learning for multiple agents faces significant challenges related to non-stationary environments and scalability. The environment appears non-stationary from the perspective of each individual agent, while the joint state-action space grows exponentially with the number of agents. Centralized training with decentralized execution (CTDE) has become a widely applied paradigm to address these issues. Many policy-based methods, e.g., MADDPG (Lowe et al. 2017), COMA (Foerster et al. 2018), FOP (Zhang et al. 2021), and value-based methods, e.g., VDN (Sunehag et al. 2017), QMIX (Rashid et al. 2020b), QPLEX (Wang et al. 2020) are proposed in this paradigm.

QMIX, a popular value-based multi-agent reinforcement learning algorithm under the CTDE paradigm, achieves state-of-the-art (SOTA) performance in the StarCraft II

Multi-Agent Challenge (SMAC (Samvelyan et al. 2019)). QMIX proposes to use a mixing function to decompose the joint action value into multiple individual action values with monotonicity constraints, ensuring consistency between the greedy actions chosen by each agent and the joint action with the maximal joint action value during decentralized execution. However, this monotonicity constraint limits the expressiveness of the mixing function, confining it to a restricted class of functions that are unable to represent arbitrary joint action values. In environments with non-monotonic reward structures, QMIX is prone to underestimating the value of the optimal joint actions (Mahajan et al. 2019), thus failing to learn the optimal policy successfully.

WQMIX (Rashid et al. 2020a) attributes this failure to the uniform weighting of all joint actions and proposes an idealized central weighting method, where the weight of the optimal joint action is higher than that of suboptimal ones. With this weighted approach, the joint action value function Q_{tot} can theoretically recover the joint action with the maximal value of any Q-learning target including the optimal joint action value function Q^*. However, traversing the entire joint action space to find the optimal joint action is computationally infeasible in practice. WQMIX proposes an approximated implementation termed Centrally-Weighted QMIX (CW-QMIX), which, however, introduces approximation error to the recognition of the optimal joint action.

To avoid the approximation error, we propose the **P**otentially **O**ptimal Joint Actions **W**eighted QMIX (POWQMIX). This algorithm defines a set of potentially optimal joint actions A_r and assigns higher weights to the joint actions within A_r. Specifically, we design a recognizer, Q_r, which functions as a joint action value function, where different Q_r values are mutually independent. It integrates individual action values with a mixing network to generate a Q_r value that determines whether a joint action belongs to A_r during training. We theoretically prove that A_r will gradually converge until it only contains the optimal joint actions and with its guidance, Q_{tot} will eventually be able to recover the optimal policy. The weighted training approach avoids the need to traverse the entire joint action space and the use of approximation methods.

Experimental results in matrix games and difficulty-enhanced predator-prey demonstrate POWQMIX's capability to cope with environments with non-monotonic reward

---

[*]These authors contributed equally.

[†]Corresponding author

structures. It achieves superior performance than the SOTA value-based methods. In SMAC benchmarks, POWQMIX also outperformed several SOTA methods in a range of tasks, proving the algorithm's scalability and robustness.

2 Background

2.1 Dec-POMDP

A cooperative multi-agent task can be modeled as a decentralized partially observable markov decision process (Dec-POMDP (Oliehoek, Amato et al. 2016)) defined by a tuple $< S, \boldsymbol{A}, O, \Omega, P, R, n, \gamma >$. $s \in S$ is the global state. After performing the joint action of n agents $\boldsymbol{a} = \{a_1, ..., a_n\}, a_i \in A_i, \boldsymbol{A} = \{A_1, ..., A_n\}$, a transition from s to the state at the next time step s' occurs according to the state transition function $P(s'|s, \boldsymbol{a})$ and all agents get a shared reward $r = R(s, \boldsymbol{a}, s')$. In partially observable scenarios, each agent can only obtain the observation $o_i \in \Omega$ of part of the environment according to the observation function $O(o_i|s)$ and has an individual policy $\pi_i(a_i|\tau_i)$ where τ_i is the action-observation history and $\boldsymbol{\tau} = \{\tau_1, ..., \tau_n\}$. The objective for solving a Dec-POMDP is to find an optimal joint policy $\boldsymbol{\pi} = \{\pi_1, ..., \pi_n\}$ to maximize the joint value function $V^{\pi}(s) = \mathbb{E}[\sum_{t=0}^{\infty} \gamma^t r_t]$.

2.2 Value Function Factorization

Value function factorization (or value decomposition) is one of the most commonly used approaches in the CTDE paradigm. Global state information is provided during training to obtain a more accurate joint action value function $Q_{tot}(\boldsymbol{\tau}, \boldsymbol{a})$ while individual action value function $Q_i(\tau_i, a_i)$ only receives its own observation to achieve full decentralization. Q_{tot} is factorized into Q_i with a mixing function f_{mix}:

$$Q_{tot} = f_{mix}(Q_1(\tau_1, a_1), ..., Q_n(\tau_n, a_n)) \qquad (1)$$

In order to ensure the consistency between joint and local greedy action selections during decentralized execution, the Individual-Global-Max (IGM) (Son et al. 2019) condition is proposed, where a global $argmax$ performed on Q_{tot} yields the same result as a set of individual $argmax$ operations performed on each Q_i:

$$(\arg\max_{a_1 \in A_1} Q_1(\tau_1, a_1), ..., \arg\max_{a_n \in A_n} Q_n(\tau_n, a_n)) = \\ \arg\max_{\boldsymbol{a} \in \boldsymbol{A}} Q_{tot}(\boldsymbol{\tau}, \boldsymbol{a}) \qquad (2)$$

The IGM condition is a necessary requirement for achieving decentralized execution. To satisfy this condition, the mixing function necessitates careful design. QMIX introduces *monotonicity constraints* between Q_{tot} and Q_i to meet this condition:

$$\frac{\partial Q_{tot}}{\partial Q_i} \geq 0, i = 1, ..., n \qquad (3)$$

To achieve the optimal consistency, the correspondence between the greedy joint action and the optimal joint action of Q^* is required, for which the True-Global-Max (TGM (Wan et al. 2021)) principle is proposed:

$$\arg\max_{\boldsymbol{a} \in \boldsymbol{A}} Q_{tot}(\boldsymbol{\tau}, \boldsymbol{a}) = \arg\max_{\boldsymbol{a} \in \boldsymbol{A}} Q^*(\boldsymbol{\tau}, \boldsymbol{a}) \qquad (4)$$

Only when the TGM condition is met can the optimal policy be recovered by Q_{tot}.

3 Related Work

The limited expressive capacity of value function factorization methods stems from the monotonicity constraints (Wang et al. 2020; Rashid et al. 2020a). And it continues to haunt as a notable concern among researchers.

QTRAN (Son et al. 2019) and QTRAN++ (Son et al. 2020) propose an unrestricted joint action value function Q_{jt} and use a transformed joint action value function $Q_{tran}(\boldsymbol{\tau}, \boldsymbol{a}) = \sum Q_i(\tau_i, a_i) + V_{jt}(s)$ to approximate Q_{jt}. $Q_{tran}(\boldsymbol{\tau}, \hat{\boldsymbol{a}})$ is constrained to be equal to $Q_{jt}(\boldsymbol{\tau}, \hat{\boldsymbol{a}})$ when $\hat{\boldsymbol{a}} = [\arg\max_{a_i \in A_i} Q_i(\tau_i, a_i)]_{i=1}^n$, and $Q_{tran}(\boldsymbol{\tau}, \boldsymbol{a}) \geq Q_{jt}(\boldsymbol{\tau}, \boldsymbol{a})$ for other joint actions. These constraints ensures to satisfy IGM, i.e. $\hat{\boldsymbol{a}} = \arg\max_{\boldsymbol{a} \in \boldsymbol{A}} Q_{jt}(\boldsymbol{\tau}, \boldsymbol{a})$. They devise multiple loss functions to achieve the aforementioned constraints. However, these loss functions cannot guarantee strict adherence to the above constraints, which may result in the violation of IGM. Additionally, V_{jt} is designed to minimize the discrepancy between Q_{jt} and $\sum Q_i(\tau_i, a_i)$. Because the input of V_{jt} is limited to s alone, it remains constant across various joint actions, lacking expressiveness. ResQ (Shen et al. 2022) decomposes Q_{jt} into a monotonicity constraints restricted component, Q_{tot}, and an unrestricted component, Q_{res}, where $Q_{jt}(\boldsymbol{\tau}, \boldsymbol{a}) = Q_{tot}(\boldsymbol{\tau}, \boldsymbol{a}) + w(s, \boldsymbol{a})Q_{res}(\boldsymbol{\tau}, \boldsymbol{a})$. $w(s, \hat{\boldsymbol{a}}) = 0$, and $w(s, \boldsymbol{a}) = 1$ for other joint actions. Q_{res} is hard-constrained to be less than or equal to 0. ResQ can be viewed as an extension of QTRAN. Q_{res} has a more powerful expressive capacity compared to V_{jt} because it additionally utilizes information from joint actions. Furthermore, ResQ strictly satisfies IGM through hard constraints on the values of Q_{res} and w.

WQMIX (Rashid et al. 2020a) introduces a weighting function when training Q_{tot} to give more importance to better joint actions. It assigns higher weights to the optimal joint action and theoretically proves that the weighted projection guarantees the recovery of the joint action with the maximal value for any Q, including Q^* as well. However, finding the optimal joint action requires traversing the entire joint action space, which is computationally impractical. To address this issue, WQMIX proposes Centrally Weighted QMIX (CW-QMIX), a practical algorithm to approximate optimal joint actions, and Optimistically Weighted QMIX (OW-QMIX), which assigns higher weights to underestimated joint actions in an optimistic identification of optimal actions. ReMIX (Mei, Zhou, and Lan 2023) formulates the optimal projection of an unrestricted mixing function onto monotonic function classes for value function factorization as a regret minimization problem. The regret is minimized by adjusting the projection weights of different state-action values. This method narrows the gap between the optimal and the restricted monotonic mixing functions.

QPLEX (Wang et al. 2020) adopts a duplex dueling architecture to satisfy the IGM condition and designs a component that incorporates joint action $\boldsymbol{a}$ as an input, fully utilizing the information from joint actions to achieve a

complete IGM function class. However, despite its capability of achieving accurate value assessments with zero loss, QPLEX may still fail to converge to the global optimum because of the instability of training and the uniform weighting of all joint actions.

Other methods, such as LICA (Zhou et al. 2020), FOP (Zhang et al. 2021), and DAVE (Xu et al. 2023), adopt a multi-agent actor-critic framework. In this framework, an unrestricted value function is employed for value function factorization, while the actor is trained through policy gradient or supervised training. These methods relax the constraints of mixing functions but cannot guarantee the strict satisfaction of the IGM condition.

4 Method

With the monotonicity constraints of the mixing function, even if one agent performs the optimal action, it is still possible to receive incorrect punishment due to the suboptimal actions performed by other agents, making it difficult to accurately estimate the values of the optimal joint actions. To address this issue, one effective strategy is to increase the weight of the optimal joint actions during training (Rashid et al. 2020a). This enhances the importance of accurately estimating the values of the optimal joint actions while reducing the incorrect punishment incurred from executing suboptimal joint actions.

To recognize the optimal joint actions, one can train an unrestricted value function and explore the entire joint action space to find the action with the highest value. Nevertheless, in MARL, the size of the joint action space grows exponentially with the number of agents, resulting in significant computational complexity and limiting its practicality to complex scenarios.

Instead of directly searching for the optimal joint actions, we propose a weighting function based on the recognition of A_r. The weighting function assigns higher weights to joint actions within A_r for QMIX. We theoretically prove that with this weighted training, A_r will converge to the optimal joint actions, enabling POWQMIX to ultimately recover the optimal policy.

4.1 Recognition of Potentially Optimal Joint Actions

The recognition module of A_r, denoted as Q_r, is a mixing function that takes individual action values, state, and joint action as inputs:

$$
\begin{aligned}
Q_r(\boldsymbol{\tau}, \boldsymbol{a}) &= f_{mix}(Q_1(\tau_1, a_1), ..., Q_n(\tau_n, a_n); s, \boldsymbol{a}) \\
&= \sum_{i=1}^{n} \lambda_i(s, \boldsymbol{a})(Q_i(\tau_i, a_i) - \max_{a_i \in A_i} Q_i(\tau_i, a_i)) \\
&\quad + V(s)
\end{aligned}
\tag{5}
$$

where the scaling function $\lambda_i(s, \boldsymbol{a}) \geq 0$.

In contrast to the mixing function employed in QMIX, Q_r integrates the joint action $\boldsymbol{a}$ as input. This allows for more comprehensive utilization of the information from joint actions and facilitates the adaptive scaling for different agents based on the specific joint action $\boldsymbol{a}$ performed by agents.

The training objective of Q_r is to approximate the optimal joint action value function Q^*. During training, updates are applied to the parameters of the mixing function, leaving the parameters of the individual action value functions unchanged.

$$
\mathcal{L}_{Q_r} = \mathbb{E}[(Q_r(\boldsymbol{\tau}, \boldsymbol{a}) - Q^*(\boldsymbol{\tau}, \boldsymbol{a}))^2]
\tag{6}
$$

Definition 1 (Potentially optimal joint actions A_r). *We define the set of joint actions that maximize the individual action value for each agent as $A_{igm} := \{\boldsymbol{a} \in \boldsymbol{A} \mid \boldsymbol{a} = [\arg\max_{a_i \in A_i} Q_i(\tau_i, a_i)]_{i=1}^n\}$. Let $\hat{\boldsymbol{a}} \in A_{igm}$. Then the set of potentially optimal joint actions A_r can be defined as:*

$$
A_r := \{\boldsymbol{a} \in \boldsymbol{A} \mid Q_r(\boldsymbol{\tau}, \boldsymbol{a}) = Q_r(\boldsymbol{\tau}, \hat{\boldsymbol{a}})\}
\tag{7}
$$

Theorem 1. *We define the set of joint actions that maximizes the optimal joint action value as $A_{tgm} := \{\boldsymbol{a} \in \boldsymbol{A} \mid \boldsymbol{a} = \arg\max_{\boldsymbol{a} \in \boldsymbol{A}} Q^*(\boldsymbol{\tau}, \boldsymbol{a})\}$. For any $\boldsymbol{\tau}$ and $\boldsymbol{a}$, let Q_r converges, we have*

$$
A_{tgm} \subseteq A_r
\tag{8}
$$

Proof. See Appendix B.

In Theorem 1, we show that the set A_r includes the optimal joint actions $\boldsymbol{a}^* \in A_{tgm}$. This condition is essential for the algorithm's capability to recover the optimal policy.

4.2 Potentially Optimal Joint Action Weighted QMIX

We introduce a weighting function $w(s, \boldsymbol{a})$ that assigns higher weights to joint actions in A_r when training an idealized QMIX with the loss function:

$$
\mathcal{L}_{Q_{tot}} = \mathbb{E}[w(s, \boldsymbol{a})(Q_{tot}(\boldsymbol{\tau}, \boldsymbol{a}) - Q^*(\boldsymbol{\tau}, \boldsymbol{a}))^2]
\tag{9}
$$

where

$$
w(s, \boldsymbol{a}) = \begin{cases} 1, \boldsymbol{a} \in A_r \\ \alpha, \boldsymbol{a} \notin A_r, \alpha \in [0, 1) \end{cases}
\tag{10}
$$

We show in Theorem 2 that with such a weighted training approach, Q_{tot} can recover the optimal policy indicated by Q^*.

Theorem 2. *Assuming that Q_{tot} has a unique maximal joint action $\hat{\boldsymbol{a}}$, there exists $\alpha = 0$ such that Q_{tot} converges with $\hat{\boldsymbol{a}} \in A_{tgm}$ and $A_r = A_{tgm}$.*

Proof. See Appendix B.

4.3 Network Architecture

The architecture of POWQMIX is shown in Figure 1. There are four key components in POWQMIX: 1) Q_{tot}, which has the same architecture as that of the fine-tuned QMIX (Hu et al. 2021). 2) An unrestricted joint action value function $\hat{Q}^*$ as in WQMIX. 3) The potentially optimal joint actions recognition module Q_r. 4) A weighting function w.

We don't have direct access to Q^* in general, but Q^* can be approximated by an unrestricted joint action value function $\hat{Q}^*$. $\hat{Q}^*$ has a similar architecture to Q_{tot} including a
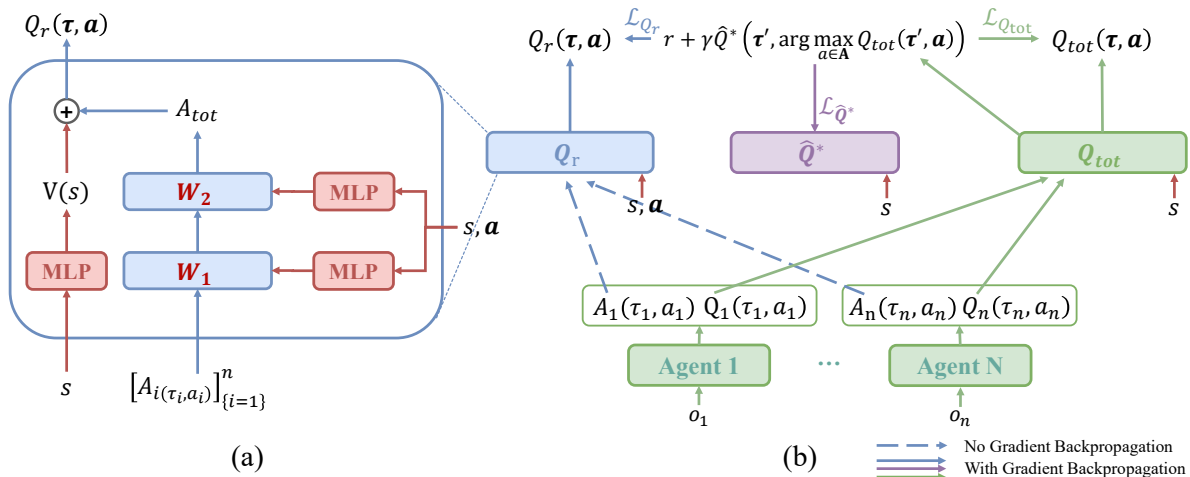
Figure 1: (a) The Q_r Network structure. (b) The overall architecture of POWQMIX.

mixing function and individual action value functions for all agents. The difference lies in the mixing function in $\hat{Q}^*$ not being constrained by monotonicity constraints.

The network architecture of Q_r is shown in Figure 1. The inputs of Q_r include three parts: the global state s, the one-hot encoding of joint action, $\boldsymbol{a}$ and the fixed values of individual advantage functions A_i. The advantage function is defined by $A_i(\tau_i, a_i) = Q_i(\tau_i, a_i) - \max_{a_i \in A_i} Q_i(\tau_i, a_i)$, and $Q_r(\boldsymbol{\tau}, \boldsymbol{a})$ is calculated by Equation 5.

The scales $\lambda_i(s, \boldsymbol{a})$ are computed by a hypernetwork, where the global state s and the joint action $\boldsymbol{a}$ are used as inputs to obtain the neural network weights W_1 and W_2. We take the absolute values of W_1 and W_2 to ensure that $\lambda_i(s, \boldsymbol{a}) \geq 0$. When $\boldsymbol{a} \in \boldsymbol{A}_{igm}$, $Q_r(\boldsymbol{\tau}, \boldsymbol{a}) = V(s)$, and when $\boldsymbol{a} \notin \boldsymbol{A}_{igm}$, $Q_r(\boldsymbol{\tau}, \boldsymbol{a}) \leq V(s)$. The input joint action $\boldsymbol{a}$ is crucial for the accurate recognition of $\boldsymbol{A}_r$. If s is the only input, there will be a monotonic relationship between $Q_r(\boldsymbol{\tau}, \boldsymbol{a})$ and $Q_i(\tau_i, a_i)$, which severely limits the representation capacity of Q_r.

Weighting Function The weighting function $w(s, \boldsymbol{a})$ is defined as:

$$w(s, \boldsymbol{a}) = \begin{cases} 1, & Q_r(\boldsymbol{\tau}, \boldsymbol{a}) \geq Q_r(\boldsymbol{\tau}, \hat{\boldsymbol{a}}) - C \\ \alpha, & \text{otherwise}, \alpha \in [0, 1) \end{cases} \tag{11}$$

where C is a small constant used for improving the stability of the recognition of $\boldsymbol{A}_r$.

$\hat{Q}^*$, Q_{tot} and Q_r share the same Q-learning target:

$$\mathcal{L}_{\hat{Q}^*} = \mathbb{E}[(\hat{Q}^*(\boldsymbol{\tau}, \boldsymbol{a}) - y)^2] \tag{12}$$

$$\mathcal{L}_{Q_{tot}} = \mathbb{E}[w(s, \boldsymbol{a})(Q_{tot}(\boldsymbol{\tau}, \boldsymbol{a}) - y)^2] \tag{13}$$

$$\mathcal{L}_{Q_r} = \mathbb{E}[(Q_r(\boldsymbol{\tau}, \boldsymbol{a}) - y)^2] \tag{14}$$

where

$$y = r + \hat{Q}^*(\boldsymbol{\tau}', \arg\max_{\boldsymbol{a} \in \boldsymbol{A}} Q_{tot}(\boldsymbol{\tau}', \boldsymbol{a})) \tag{15}$$

If Q_{tot} can recover the joint action with the maximal value of $\hat{Q}^*$, that is, when $\arg\max_{\boldsymbol{a} \in \boldsymbol{A}} Q_{tot}(\boldsymbol{\tau}', \boldsymbol{a}) =$

$\arg\max_{\boldsymbol{a} \in \boldsymbol{A}} \hat{Q}^*(\boldsymbol{\tau}', \boldsymbol{a})$, $\hat{Q}^*$ becomes the optimal joint action value function Q^*. Although Theorem 2 proves that Q_{tot} is capable of recovering the optimal policy of Q^*, in fact, this holds true for any arbitrary Q, naturally including $\hat{Q}^*$.

5 Experiment

In this section, we evaluate the performance of POWQMIX and other SOTA algorithms across matrix games and difficulty-enhanced predator-prey, both of which exhibit strong non-monotonicity, aligning well with the specific challenges our algorithm is designed to address. Additionally, we assess their performance in the SMAC environment, which, despite its weaker non-monotonicity, is widely recognized as a complex and rigorous benchmark for MARL. All algorithms and experiments are conducted based on the PyMARL2 (Hu et al. 2021) framework, where hyperparameters such as the type of optimizer and replay buffer size are finely tuned. More details about the algorithms and experimental hyperparameters are provided in Appendix D. All results are obtained from 5 runs under different random seeds and are plotted using means and standard deviation with 95% confidence intervals.

5.1 Matrix Game

We test the representation capacity of several algorithms in a matrix game environment with very strong non-monotonicity in the reward structure, which is consistent with the setting in the ResQ paper. To eliminate the impact of exploration and randomness from sampling, we set $\epsilon = 1$ for $\epsilon - greedy$ to ensure a uniform data distribution. We record the individual and joint action values after convergence, as shown in Table 1. POWQMIX, CW-QMIX, and ResQ algorithms can recover the optimal policy. In POWQMIX, thanks to the powerful expressiveness of the Q_r module, all joint action Q_r values are accurately estimated, allowing the optimal joint action to be precisely recognized and used for weighted training. Although QPLEX converges to local optima, its assessment of the optimal joint action value tends

A_1 \ A_2	**A**	**B**	**C**
A	**8**	-12	-12
B	-12	0	0
C	-12	0	7.9

(a) Payoff Matrix

Q_1 \ Q_2	**0.060(A)**	-0.160(B)	-0.045(C)
0.041(A)	**8.00**	7.95	7.97
-0.150(B)	7.95	7.90	7.93
-0.051(C)	7.98	7.92	7.95

(b) POWQMIX: Q_1, Q_2, Q_{tot}

Q_1 \ Q_2	**0.060(A)**	-0.160(B)	-0.045(C)
0.041(A)	**8.00**	-12.00	-12.00
-0.150(B)	-12.00	0.00	0.00
-0.051(C)	-12.00	0.00	7.90

(c) POWQMIX: Q_1, Q_2, Q_r

Q_1 \ Q_2	-22.90(A)	-0.132(B)	**0.092(C)**
-23.23(A)	-8.11	-8.10	-8.11
-0.141(B)	-8.10	-0.33	0.15
0.091(C)	-8.10	0.16	**7.90**

(d) QMIX: Q_1, Q_2, Q_{tot}

Q_1 \ Q_2	0.814(A)	0.133((B)	**0.912(C)**
0.835(A)	16.27	12.67	16.70
0.120(B)	13.21	9.62	13.63
0.906(C)	16.37	12.77	**16.79**

(e) OW-QMIX: Q_1, Q_2, Q_{tot}

Q_1 \ Q_2	**0.060(A)**	-0.160(B)	-0.045(C)
0.041(A)	**8.00**	7.95	7.97
-0.150(B)	7.95	7.90	7.93
-0.051(C)	7.98	7.92	7.95

(f) CW-QMIX: Q_1, Q_2, Q_{tot}

Q_1 \ Q_2	-0.319(A)	-1.205(B)	**0.004(C)**
-0.314(A)	9.68	-12.77	-14.52
-1.100(B)	-12.04	-0.32	-0.08
-0.006(C)	-10.64	-0.38	**9.69**

(g) QPLEX: Q_1, Q_2, Q_{tot}

Q_1 \ Q_2	**0.109(A)**	-0.325(B)	0.105(C)
0.105(A)	**7.982**	7.792	7.976
-0.316(B)	7.818	7.630	7.811
0.101(C)	7.976	7.786	7.969

(h) ResQ: Q_1, Q_2, Q_{tot}

Q_1 \ Q_2	**0.100(A)**	-0.303(B)	0.091(C)
0.099(A)	**7.98**	-12.22	-12.22
-0.298(B)	-12.27	-0.08	-0.09
0.089(C)	-12.29	-0.08	7.91

(i) ResQ: Q_1, Q_2, Q_{jt}

Table 1: Payoff matrix of a one-step matrix game and reconstructed joint and individual values. Boldface means greedy actions. Blue color indicates the true optimal joint action, whereas red color represents a suboptimal joint action.
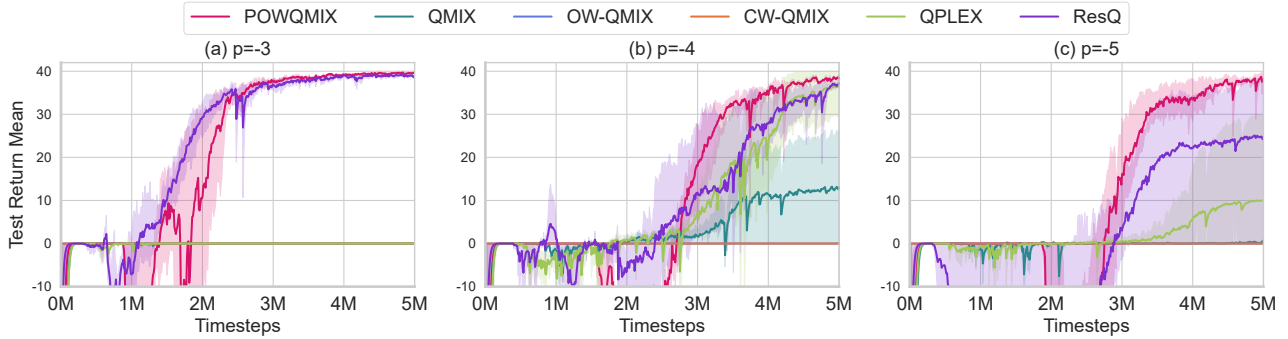
Figure 2: Test return in Predator-Prey with three different mis-capture punishment.

to be as high as possible, and the values of the remaining joint actions are accurately estimated, which is an important inspiration for us to design the Q_r module.

5.2 Predator-Prey

In the predator-prey environment, the predators, acting as agents, need to collaborate to capture prey. When only one agent attempts to perform the *capture* action, all agents receive a mis-capture punishment p. The greater the punishment, the stronger the non-monotonicity of the reward structure, and the more likely the agents are to learn a passive strategy, i.e., never performing the *capture* action. The experimental results under three different levels of mis-capture punishment are shown in Figure 2. POWQMIX is the only algorithm that consistently learns the optimal policy across all settings.

5.3 SMAC

We evaluate the performance of all algorithms on six SMAC maps, including one easy map, one hard maps, and four super-hard maps. Experimental results in Figure 3 show that

POWQMIX demonstrates excellent performance across various scenarios. The PyMARL2 (Hu et al. 2021) characterize SMAC as a purely cooperative task environment, which suggests that SMAC exhibits weak non-monotonic characteristics. Despite the focus of our improvement on addressing non-monotonicity, it still demonstrates commendable performance within this complex and widely recognized environment. CW-QMIX, while theoretically capable of finding the optimal policy in matrix games, underperforms in many SMAC scenarios, showing its limited scalability. QPLEX experiences several performance drops during training, possibly related to its training instability caused by the dueling architecture. Although OW-QMIX performs well in the SMAC environment, it cannot theoretically recover the optimal policy, as shown in Table 1.

5.4 Ablation

Based on Equation 11 and Theorem 2, as well as the fact that increasing the weight of the loss does not change the magnitude of the final parameter update when using the Adam optimizer, we set the weight for potentially optimal joint ac-
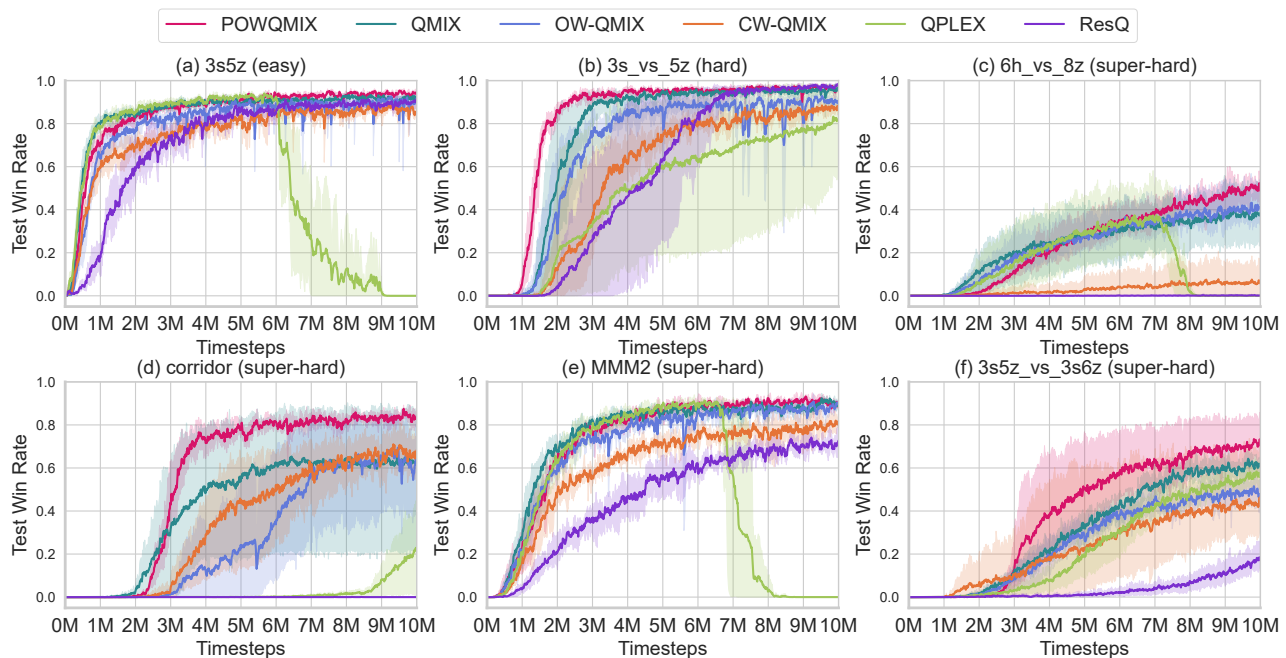
Figure 3: Test win rate of the SMAC benchmarks.

tions to 5 and for other joint actions to 0 in the POWQMIX implementation. While this approach is theoretically sound, it may raise concerns, and the gradient clipping in the py-marl2 framework could cause larger weights to more easily hit the gradient limit, potentially introducing disturbances into training.

To address this, we first tested POWQMIX's sensitivity to different weights to ensure robustness. Then, we applied the weights of 5 to the baselines to assess their performance when deviating from their default settings.

Weight Sensitivity We run experiments to test the sensitivity of POWQMIX to different weights. The experimental results are shown in Figure 4 with the labels of various ablation methods where the first digit represents the weights of the potentially optimal joint actions, and the second digit represents the weights of other joint actions. The experimental results demonstrate the strong robustness of POWQMIX, as evidenced by the fact that, although there are differences in the convergence speed, the final average performance remains largely consistent. Additionally, while assigning weights to other joint actions slightly improves performance in the predator-prey environment, this effect is not observed in SMAC. The appropriate weighting settings vary for different environments. To be in line with theoretical conformance (where $\alpha = 0$) and consistent performance, we opt for the weight configuration (5,0) for the implementation of the algorithm.

Weighting Comparison In this section, we adjust the weights in QMIX, CW-QMIX, and OW-QMIX during comparative experiments. In QMIX-5, the weight for all joint actions is set to 5. In CW-QMIX-5 and OW-QMIX-5, the weight assigned to the optimal joint action is 5, while other

joint actions are assigned a weight of 0, consistent with our algorithm.

The experimental results are shown in Figure 5. With a larger weight, QMIX-5 shows improved performance on SMAC, indicating that in scenarios where non-monotonicity is not strongly pronounced, higher weights lead to more stable performance and an overall increase in average return. However, its performance on the predator-prey environment remains largely unchanged, suggesting that simply increasing weights does not enhance performance in environments with significant non-monotonic characteristics. Conversely, CW-QMIX-5 shows improved results in the predator-prey setting but experiences a decline in SMAC performance. This suggests that while greater perturbations in simpler environments can help agents escape local optima, they do not translate to better performance in more complex settings. OW-QMIX-5 continues to perform poorly in predator-prey and drops to zero on the corridor map, indicating that the training weights associated with suboptimal joint actions are also critical for OW-QMIX to successfully learn and adapt.

Parameter Count In value decomposition methods designed to overcome monotonicity constraints, the inclusion of Q_{tot} and $\hat{Q}^*$ is essential. Our additional potentially optimal joint actions recognition module, Q_r, adds complexity to the algorithm. To determine whether the observed performance improvements stem from increased complexity and parameter count, we standardized the parameter count across all algorithms with similar modules. The results are shown in Figure 6. For CW-QMIX and OW-QMIX, the expanded networks improve performance in the predator-prey environment but hinder it in SMAC. QPLEX, however, perform poorly across all tasks. The enhanced QMIX showed
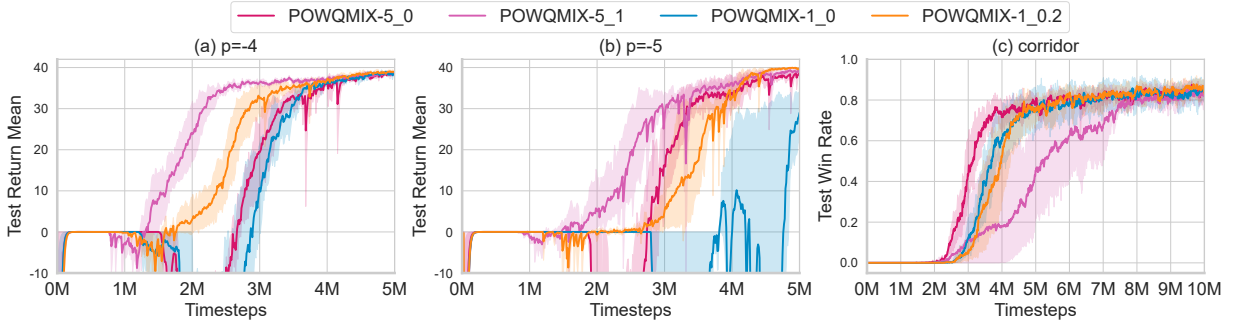
Figure 4: Ablation results of sensitivity to different weights for POWQMIX. (a) and (b) show the performance comparison in difficulty-enhanced predator-prey with $p = -4$ and $p = -5$, and (c) on a SMAC map.
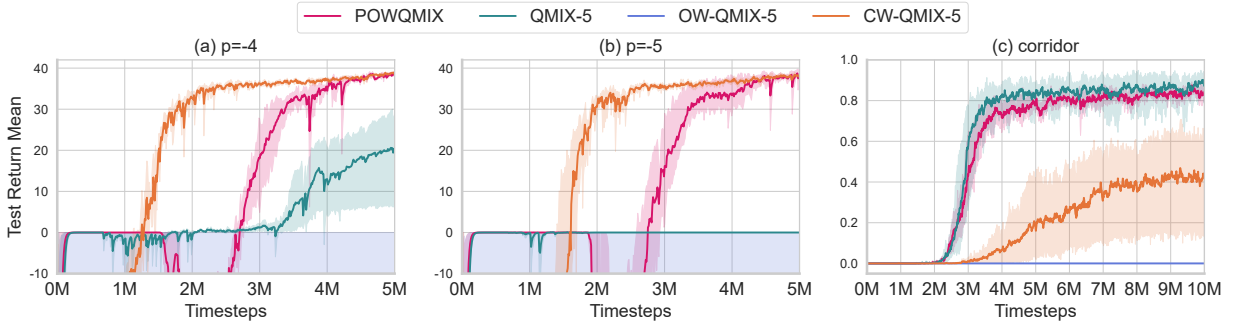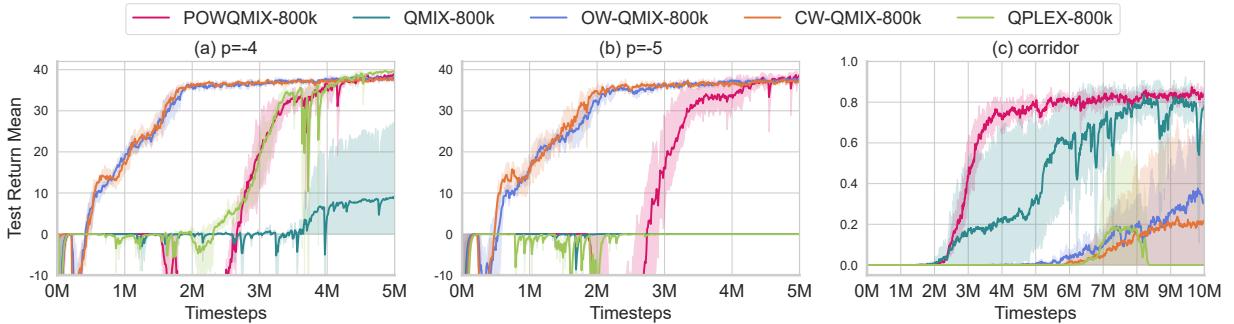

Figure 5: Ablation results of different weights in weighting functions for POWQMIX and other baseline algorithms. (a) and (b) show the performance comparison in difficulty-enhanced predator-prey with $p = -4$ and $p = -5$, and (c) on a SMAC map.

Figure 6: Ablation results of network size. (a) and (b) show the performance comparison in difficulty-enhanced predator-prey with $p = -4$ and $p = -5$, and (c) on a SMAC map.

improved performance in SMAC, where non-monotonicity is less of an issue, but still struggled in the predator-prey environment due to its inherent monotonic constraints.

We believe that our network design effectively addresses non-monotonic issues, as evidenced by its performance in matrix games and predator-prey scenarios. The ability to maintain benchmark performance in SMAC while significantly improving in non-monotonic scenarios suggests that the additional module is indeed worthwhile.

6 Conclusions and Limitations

This paper presented POWQMIX, a weighted training method based on potentially optimal joint actions. POWQMIX employs a Q_r module to determine whether a joint action is a potentially optimal one and assigns appropriate weights during training. We formally prove that with this weighted training, the set of potentially optimal joint actions will eventually converge to the actual optimal joint actions, and Q_{tot} can recover the optimal policy. Experimental results in multiple environments fully validate the theoretical effectiveness and superior performance of POWQMIX. However, due to the introduction of additional modules pro-

posed by POWQMIX to address non-monotonicity issues, the training process becomes more complex. Therefore, reducing the computation burden of POWQMIX in complex environments is considered as our future work.

References

Foerster, J.; Farquhar, G.; Afouras, T.; Nardelli, N.; and Whiteson, S. 2018. Counterfactual multi-agent policy gradients. In *Proceedings of the AAAI conference on artificial intelligence*, volume 32.

Hu, J.; Jiang, S.; Harding, S. A.; Wu, H.; and Liao, S.-w. 2021. Rethinking the implementation tricks and monotonicity constraint in cooperative multi-agent reinforcement learning. *arXiv preprint arXiv:2102.03479*.

Huang, Y.; Wu, S.; Mu, Z.; Long, X.; Chu, S.; and Zhao, G. 2020. A multi-agent reinforcement learning method for swarm robots in space collaborative exploration. In *2020 6th international conference on control, automation and robotics (ICCAR)*, 139–144. IEEE.

Lowe, R.; Wu, Y. I.; Tamar, A.; Harb, J.; Pieter Abbeel, O.; and Mordatch, I. 2017. Multi-agent actor-critic for mixed cooperative-competitive environments. *Advances in neural information processing systems*, 30.

Mahajan, A.; Rashid, T.; Samvelyan, M.; and Whiteson, S. 2019. Maven: Multi-agent variational exploration. *Advances in neural information processing systems*, 32.

Mei, Y.; Zhou, H.; and Lan, T. 2023. Remix: Regret minimization for monotonic value function factorization in multiagent reinforcement learning. *arXiv preprint arXiv:2302.05593*.

Oliehoek, F. A.; Amato, C.; et al. 2016. *A concise introduction to decentralized POMDPs*, volume 1. Springer.

Rashid, T.; Farquhar, G.; Peng, B.; and Whiteson, S. 2020a. Weighted qmix: Expanding monotonic value function factorisation for deep multi-agent reinforcement learning. *Advances in neural information processing systems*, 33: 10199–10210.

Rashid, T.; Samvelyan, M.; De Witt, C. S.; Farquhar, G.; Foerster, J.; and Whiteson, S. 2020b. Monotonic value function factorisation for deep multi-agent reinforcement learning. *The Journal of Machine Learning Research*, 21(1): 7234–7284.

Samvelyan, M.; Rashid, T.; De Witt, C. S.; Farquhar, G.; Nardelli, N.; Rudner, T. G.; Hung, C.-M.; Torr, P. H.; Foerster, J.; and Whiteson, S. 2019. The starcraft multi-agent challenge. *arXiv preprint arXiv:1902.04043*.

Schmidt, L. M.; Brosig, J.; Plinge, A.; Eskofier, B. M.; and Mutschler, C. 2022. An introduction to multi-agent reinforcement learning and review of its application to autonomous mobility. In *2022 IEEE 25th International Conference on Intelligent Transportation Systems (ITSC)*, 1342–1349. IEEE.

Shen, S.; Qiu, M.; Liu, J.; Liu, W.; Fu, Y.; Liu, X.; and Wang, C. 2022. ResQ: A Residual Q Function-based Approach for Multi-Agent Reinforcement Learning Value Factorization. *Advances in Neural Information Processing Systems*, 35: 5471–5483.

Son, K.; Ahn, S.; Reyes, R. D.; Shin, J.; and Yi, Y. 2020. QTRAN++: improved value transformation for cooperative multi-agent reinforcement learning. *arXiv preprint arXiv:2006.12010*.

Son, K.; Kim, D.; Kang, W. J.; Hostallero, D. E.; and Yi, Y. 2019. Qtran: Learning to factorize with transformation for cooperative multi-agent reinforcement learning. In *International conference on machine learning*, 5887–5896. PMLR.

Sunehag, P.; Lever, G.; Gruslys, A.; Czarnecki, W. M.; Zambaldi, V.; Jaderberg, M.; Lanctot, M.; Sonnerat, N.; Leibo, J. Z.; Tuyls, K.; et al. 2017. Value-decomposition networks for cooperative multi-agent learning. *arXiv preprint arXiv:1706.05296*.

Terry, J.; Black, B.; Grammel, N.; Jayakumar, M.; Hari, A.; Sullivan, R.; Santos, L. S.; Dieffendahl, C.; Horsch, C.; Perez-Vicente, R.; et al. 2021. Pettingzoo: Gym for multi-agent reinforcement learning. *Advances in Neural Information Processing Systems*, 34: 15032–15043.

Wan, L.; Liu, Z.; Chen, X.; Wang, H.; and Lan, X. 2021. Greedy-based value representation for optimal coordination in multi-agent reinforcement learning. *arXiv preprint arXiv:2112.04454*.

Wang, J.; Ren, Z.; Liu, T.; Yu, Y.; and Zhang, C. 2020. Qplex: Duplex dueling multi-agent q-learning. *arXiv preprint arXiv:2008.01062*.

Xu, Z.; Zhang, B.; Li, D.; Zhou, G.; Zhang, Z.; and Fan, G. 2023. Dual Self-Awareness Value Decomposition Framework without Individual Global Max for Cooperative Multi-Agent Reinforcement Learning. *arXiv preprint arXiv:2302.02180*.

Zhang, T.; Li, Y.; Wang, C.; Xie, G.; and Lu, Z. 2021. Fop: Factorizing optimal joint policy of maximum-entropy multi-agent reinforcement learning. In *International Conference on Machine Learning*, 12491–12500. PMLR.

Zhou, M.; Liu, Z.; Sui, P.; Li, Y.; and Chung, Y. Y. 2020. Learning implicit credit assignment for cooperative multi-agent reinforcement learning. *Advances in neural information processing systems*, 33: 11853–11864.

Appendix

A   Relationship to Related Works

We compare the similarities and differences between POWQMIX and the most relevant algorithms.

Relation to WQMIX WQMIX proposes CW-QMIX, which assigns higher weights to the optimal joint actions. It makes approximations when computing the optimal joint actions, which reduces complexity at the expense of introducing approximation errors. POWQMIX proposes a weighting function based on potentially optimal joint actions. Through iterative training, we gradually narrow down the range of $\boldsymbol{A}_r$ until the optimal joint actions are found. Therefore, there is no need to explicitly find the optimal joint actions by traversing the whole joint action space or making some approximations.

Relation to QPLEX QPLEX introduces the duplex dueling architecture based on the advantage function $Q_i(\tau_i, a_i) - \max_{a \in A_i} Q_i(\tau_i, a)$ and a $\lambda(s, \boldsymbol{a})$ network incorporating the joint action $\boldsymbol{a}$ as an input. It constructs a complete IGM function class without imposing additional constraints like monotonicity to the mixing function, theoretically achieving zero-loss convergence of multi-agent Q-learning to the optimal solution. However, in practical applications, the simultaneous training of both the λ network and individual action value functions Q_i increases the variations of joint action value assessment, leading to instability problems. POWQMIX trains the λ network in Q_r based on the fixed values of Q_i, without simultaneously training the networks of Q_i. This enhances stability while fully utilizing the representational capability of the λ network to effectively recognize potentially optimal joint actions.

Relation to ResQ ResQ uses the sum of two joint action value functions: Q_{tot} with monotonicity constraints and a residual value function Q_{res} without monotonicity constraints, to estimate the optimal joint action value. The residual value Q_{res}, constrained to be less than or equal to zero, will strive to increase to zero when the optimal joint action value is higher than that assessed by Q_{tot}. This characteristic echoes the principles of the recognition module Q_r utilized in POWQMIX. However, unlike our approach, the detailed proofs of such mechanisms were not articulated in the ResQ paper. Moreover, although ResQ is guaranteed to recover the optimal policy, it assigns equal importance to the estimation of all joint action values and the training signals from suboptimal joint actions can interfere with the process of learning the optimal policy. POWQMIX focuses more on potentially optimal joint actions and can reduce interference from suboptimal actions, allowing the algorithm to learn the optimal policy more steadily.

Besides these SOTA algorithms, several other methods are in value decomposition domain, including ReMIX and ConcaveQ. However, since they do not have open-source code available, we did not include these two methods as baselines in our paper. As for the classic QTRAN, due to its poor scalability, as evidenced by experimental results in WQMIX and QPLEX, it is not considered as a baseline in this paper.

B   Proof of Theorems

Lemma 1.   For any $\boldsymbol{\tau}$ and joint action $\boldsymbol{a} \notin \boldsymbol{A}_{igm}$, let Q_r has converged, it holds that

$$Q_r(\boldsymbol{\tau}, \boldsymbol{a}) = \min(Q_r(\boldsymbol{\tau}, \hat{\boldsymbol{a}}), Q^*(\boldsymbol{\tau}, \boldsymbol{a}))$$

Proof. According to the definition of Q_r, for $\boldsymbol{a} \notin \boldsymbol{A}_{igm}$, it satisfies

$$Q_r(\boldsymbol{\tau}, \boldsymbol{a}) \leq Q_r(\boldsymbol{\tau}, \hat{\boldsymbol{a}})$$

For each joint action $\boldsymbol{a}$, the corresponding objective function is $\mathcal{L}_{Q_r}(\boldsymbol{\tau}, \boldsymbol{a}) = (Q_r(\boldsymbol{\tau}, \boldsymbol{a}) - Q^*(\boldsymbol{\tau}, \boldsymbol{a}))^2$. Consider two cases:

- $Q^*(\boldsymbol{\tau}, \boldsymbol{a}) \geq Q_r(\boldsymbol{\tau}, \hat{\boldsymbol{a}})$:
  In this case, $(Q_r(\boldsymbol{\tau}, \boldsymbol{a}) - Q^*(\boldsymbol{\tau}, \boldsymbol{a}))^2 \geq (Q_r(\boldsymbol{\tau}, \hat{\boldsymbol{a}}) - Q^*(\boldsymbol{\tau}, \boldsymbol{a}))^2$. To minimize $\mathcal{L}_{Q_r}(\boldsymbol{\tau}, \boldsymbol{a})$, $Q_r(\boldsymbol{\tau}, \boldsymbol{a})$ should be maximized. Therefore, $Q_r(\boldsymbol{\tau}, \boldsymbol{a}) = Q_r(\boldsymbol{\tau}, \hat{\boldsymbol{a}}) = \min(Q_r(\boldsymbol{\tau}, \hat{\boldsymbol{a}}), Q^*(\boldsymbol{\tau}, \boldsymbol{a}))$.

- $Q^*(\boldsymbol{\tau}, \boldsymbol{a}) < Q_r(\boldsymbol{\tau}, \hat{\boldsymbol{a}})$:
  When $Q_r(\boldsymbol{\tau}, \boldsymbol{a}) = Q^*(\boldsymbol{\tau}, \boldsymbol{a})$, $\mathcal{L}_{Q_r}(\boldsymbol{\tau}, \boldsymbol{a}) = 0$, which also satisfies $Q_r(\boldsymbol{\tau}, \boldsymbol{a}) = \min(Q_r(\boldsymbol{\tau}, \hat{\boldsymbol{a}}), Q^*(\boldsymbol{\tau}, \boldsymbol{a}))$.

Combining these two cases confirms Lemma 1.

Lemma 2.   Let Q_r has converged, it satisfies

$$Q_r(\boldsymbol{\tau}, \hat{\boldsymbol{a}}) \leq Q^*(\boldsymbol{\tau}, \boldsymbol{a}^*)$$

Proof. Assume for a contradiction that

$$Q_r(\boldsymbol{\tau}, \hat{\boldsymbol{a}}) > Q^*(\boldsymbol{\tau}, \boldsymbol{a}^*)$$

According to Lemma 1, for joint actions $\boldsymbol{a} \notin \boldsymbol{A}_{igm}$, it holds that

$$Q_r(\boldsymbol{\tau}, \boldsymbol{a}) = \min(Q_r(\boldsymbol{\tau}, \hat{\boldsymbol{a}}), Q^*(\boldsymbol{\tau}, \boldsymbol{a})) = Q^*(\boldsymbol{\tau}, \boldsymbol{a})$$

Construct Q'_r based on Q_r:

$$Q'_r(\boldsymbol{\tau}, \boldsymbol{a}) = \begin{cases} Q^*(\boldsymbol{\tau}, \boldsymbol{a}^*), & \boldsymbol{a} \in \boldsymbol{A}_{igm} \\ Q_r(\boldsymbol{\tau}, \boldsymbol{a}), & \boldsymbol{a} \notin \boldsymbol{A}_{igm} \end{cases}$$

Construct the simplified objective function $\mathcal{L}_{Q'_r}$ corresponding to Q'_r:

$$
\begin{aligned}
\mathcal{L}_{Q'_r} &= \sum_{\boldsymbol{a} \in \boldsymbol{A}_r} (Q'_r(\boldsymbol{\tau}, \boldsymbol{a}) - Q^*(\boldsymbol{\tau}, \boldsymbol{a}))^2 + \sum_{\boldsymbol{a} \notin \boldsymbol{A}_r} (Q_r(\boldsymbol{\tau}, \boldsymbol{a}) - Q^*(\boldsymbol{\tau}, \boldsymbol{a}))^2 \\
&= \sum_{\boldsymbol{a} \in \boldsymbol{A}_r} (Q'_r(\boldsymbol{\tau}, \boldsymbol{a}) - Q^*(\boldsymbol{\tau}, \boldsymbol{a}))^2 \\
&= \sum_{\boldsymbol{a} \in \boldsymbol{A}_r \cap \boldsymbol{A}_{igm}} (Q'_r(\boldsymbol{\tau}, \boldsymbol{a}) - Q^*(\boldsymbol{\tau}, \boldsymbol{a}))^2 + \sum_{\boldsymbol{a} \in \boldsymbol{A}_r \setminus \boldsymbol{A}_{igm}} (Q_r(\boldsymbol{\tau}, \boldsymbol{a}) - Q^*(\boldsymbol{\tau}, \boldsymbol{a}))^2 \\
&= \sum_{\boldsymbol{a} \in \boldsymbol{A}_r \cap \boldsymbol{A}_{igm}} (Q^*(\boldsymbol{\tau}, \boldsymbol{a}^*) - Q^*(\boldsymbol{\tau}, \boldsymbol{a}))^2 + \sum_{\boldsymbol{a} \in \boldsymbol{A}_r \setminus \boldsymbol{A}_{igm}} (Q_r(\boldsymbol{\tau}, \boldsymbol{a}) - Q^*(\boldsymbol{\tau}, \boldsymbol{a}))^2 \\
&< \sum_{\boldsymbol{a} \in \boldsymbol{A}_r \cap \boldsymbol{A}_{igm}} (Q_r(\boldsymbol{\tau}, \hat{\boldsymbol{a}}) - Q^*(\boldsymbol{\tau}, \boldsymbol{a}))^2 + \sum_{\boldsymbol{a} \in \boldsymbol{A}_r \setminus \boldsymbol{A}_{igm}} (Q_r(\boldsymbol{\tau}, \boldsymbol{a}) - Q^*(\boldsymbol{\tau}, \boldsymbol{a}))^2 \\
&= \mathcal{L}_{Q_r}
\end{aligned}
$$

Thus, $\mathcal{L}_{Q'_r} < \mathcal{L}_{Q_r}$, when Q_r has fully converged, the condition $Q_r(\boldsymbol{\tau}, \hat{\boldsymbol{a}}) > Q^*(\boldsymbol{\tau}, \boldsymbol{a}^*)$ cannot be satisfied. By contradiction, it can be known that Lemma 2 holds.

Theorem 1. For any $\boldsymbol{\tau}$ and $\boldsymbol{a}$, let Q_r has converged, we have

$$\boldsymbol{A}_{tgm} \subseteq \boldsymbol{A}_r$$

Proof. According to Lemma 1 and 2, for any $\boldsymbol{a}^* \in \boldsymbol{A}_{tgm}$, we have
- When $\boldsymbol{a}^* \in \boldsymbol{A}_{igm}$: as $\boldsymbol{A}_{igm} \subseteq \boldsymbol{A}_r$, therefore, $\boldsymbol{a}^* \in \boldsymbol{A}_r$
- When $\boldsymbol{a}^* \notin \boldsymbol{A}_{igm}$: $Q_r(\boldsymbol{\tau}, \boldsymbol{a}^*) = \min(Q_r(\boldsymbol{\tau}, \hat{\boldsymbol{a}}), Q^*(\boldsymbol{\tau}, \boldsymbol{a}^*)) = Q_r(\boldsymbol{\tau}, \hat{\boldsymbol{a}})$, therefore, $\boldsymbol{a}^* \in \boldsymbol{A}_r$.

As for any $\boldsymbol{a}^* \in \boldsymbol{A}_{tgm}$, we have $\boldsymbol{a}^* \in \boldsymbol{A}_r$, therefore, $\boldsymbol{A}_{tgm} \subseteq \boldsymbol{A}_r$.

Lemma 3. When Q_r has converged, if $\boldsymbol{A}_{igm} \subseteq \boldsymbol{A}_{tgm}$, then $Q_r(\boldsymbol{\tau}, \hat{\boldsymbol{a}}) = Q^*(\boldsymbol{\tau}, \boldsymbol{a}^*)$. If $\boldsymbol{A}_{igm} \nsubseteq \boldsymbol{A}_{tgm}$, then $\min_{\boldsymbol{a} \in \boldsymbol{A}_{igm}} Q^*(\boldsymbol{\tau}, \boldsymbol{a}) < Q_r(\boldsymbol{\tau}, \hat{\boldsymbol{a}}) < Q^*(\boldsymbol{\tau}, \boldsymbol{a}^*)$.

Proof.
- If $\boldsymbol{A}_{igm} \subseteq \boldsymbol{A}_{tgm}$, then when $Q_r(\boldsymbol{\tau}, \hat{\boldsymbol{a}}) = Q^*(\boldsymbol{\tau}, \boldsymbol{a}^*)$, $\mathcal{L}_{Q_r} = 0$. When $Q_r(\boldsymbol{\tau}, \hat{\boldsymbol{a}}) \neq Q^*(\boldsymbol{\tau}, \boldsymbol{a}^*)$, $\mathcal{L}_{Q_r} > 0$, thus $Q_r(\boldsymbol{\tau}, \hat{\boldsymbol{a}}) = Q^*(\boldsymbol{\tau}, \boldsymbol{a}^*)$ holds true.
- If $\boldsymbol{A}_{igm} \nsubseteq \boldsymbol{A}_{tgm}$, divide the loss function $\mathcal{L}_{Q_r}$ into two parts $\mathcal{L}_1$ and $\mathcal{L}_2$ based on the categories of joint actions $\boldsymbol{a} \in \boldsymbol{A}_{igm} \cup \boldsymbol{A}_{tgm}$ and $\boldsymbol{a} \notin \boldsymbol{A}_{igm} \cup \boldsymbol{A}_{tgm}$. According to Lemma 1 and Lemma 2, for $\boldsymbol{a} \in \boldsymbol{A}_{igm} \cup \boldsymbol{A}_{tgm}$, $Q_r(\boldsymbol{\tau}, \boldsymbol{a}) = Q_r(\boldsymbol{\tau}, \hat{\boldsymbol{a}})$.

$$
\begin{aligned}
\mathcal{L}_{Q_r} &= \mathcal{L}_1 + \mathcal{L}_2 \\
&= \sum_{\boldsymbol{a} \in \boldsymbol{A}_{igm} \cup \boldsymbol{A}_{tgm}} (Q_r(\boldsymbol{\tau}, \boldsymbol{a}) - Q^*(\boldsymbol{\tau}, \boldsymbol{a}))^2 + \sum_{\boldsymbol{a} \notin \boldsymbol{A}_{igm} \cup \boldsymbol{A}_{tgm}} (Q_r(\boldsymbol{\tau}, \boldsymbol{a}) - Q^*(\boldsymbol{\tau}, \boldsymbol{a}))^2 \\
&= \sum_{\boldsymbol{a} \in \boldsymbol{A}_{igm} \cup \boldsymbol{A}_{tgm}} (Q_r(\boldsymbol{\tau}, \hat{\boldsymbol{a}}) - Q^*(\boldsymbol{\tau}, \boldsymbol{a}))^2 + \sum_{\boldsymbol{a} \notin \boldsymbol{A}_{igm} \cup \boldsymbol{A}_{tgm}} (Q_r(\boldsymbol{\tau}, \boldsymbol{a}) - Q^*(\boldsymbol{\tau}, \boldsymbol{a}))^2
\end{aligned}
$$

Consider $\mathcal{L}_1$, since $\boldsymbol{A}_{igm} \nsubseteq \boldsymbol{A}_{tgm}$, it is evident that $\min_{\boldsymbol{a} \in \boldsymbol{A}_{igm}} Q^*(\boldsymbol{\tau}, \boldsymbol{a}) < Q^*(\boldsymbol{\tau}, \boldsymbol{a}^*)$. Consider $\mathcal{L}_1$ as a quadratic function with the variable $Q_r(\boldsymbol{\tau}, \hat{\boldsymbol{a}})$ and define when $Q_r(\boldsymbol{\tau}, \hat{\boldsymbol{a}}) = m$, $\mathcal{L}_1$ reaches its minimum value. By the properties of quadratic functions, it can be known that, $\min_{\boldsymbol{a} \in \boldsymbol{A}_{igm}} Q^*(\boldsymbol{\tau}, \boldsymbol{a}) < m < Q^*(\boldsymbol{\tau}, \boldsymbol{a}^*)$, and the interval $(-\infty, m)$ marks a monotonic decrease in $\mathcal{L}_1$ with respect to $Q_r(\boldsymbol{\tau}, \hat{\boldsymbol{a}})$, whereas $(m, +\infty)$ signifies a monotonic increase.

Consider $\mathcal{L}_2$, where joint actions $\boldsymbol{a} \notin \boldsymbol{A}_{igm} \cup \boldsymbol{A}_{tgm}$. Consider again $\mathcal{L}_2$ as a quadratic function with the variable $Q_r(\boldsymbol{\tau}, \hat{\boldsymbol{a}})$ and define $\max_{\boldsymbol{a} \notin \boldsymbol{A}_{igm} \cup \boldsymbol{A}_{tgm}} Q^*(\boldsymbol{\tau}, \boldsymbol{a}) = n$, it is evident that $n < Q^*(\boldsymbol{\tau}, \boldsymbol{a}^*)$. According to Lemma 1, it can be known that the interval $(-\infty, n)$ marks a monotonic decrease in $\mathcal{L}_2$ with respect to $Q_r(\boldsymbol{\tau}, \hat{\boldsymbol{a}})$ and $\mathcal{L}_2 = 0$ in the interval $(n, +\infty)$.

The combination of the monotonic intervals of $\mathcal{L}_1$ and $\mathcal{L}_2$ shows that $\mathcal{L}_{Q_r}$ strictly decreases in the interval $(\min_{\boldsymbol{a} \in \boldsymbol{A}_{igm}} Q^*(\boldsymbol{\tau}, \boldsymbol{a}), m)$ and strictly increases in the interval $(n, Q^*(\boldsymbol{\tau}, \boldsymbol{a}^*))$.

The strict monotonic intervals of $\mathcal{L}_{Q_r}$ demonstrate that $\min_{\boldsymbol{a} \in \boldsymbol{A}_{igm}} Q^*(\boldsymbol{\tau}, \boldsymbol{a}) < Q_r(\boldsymbol{\tau}, \hat{\boldsymbol{a}}) < Q^*(\boldsymbol{\tau}, \boldsymbol{a}^*)$.

The combination of the above two cases completes the proof of Lemma 3.

Theorem 2. Assuming that Q_{tot} has a unique maximal joint action $\hat{a}$, there exists $\alpha = 0$ such that Q_{tot} converges with $\hat{a} \in A_{tgm}$ and $A_r = A_{tgm}$.

Proof. To deduce the lower bound of $\mathcal{L}_{Q_{tot}}$, we categorize $\mathcal{L}_{Q_{tot}}$ into four types based on the categories and values of joint actions:

$$\mathcal{L}_{Q_{tot}} = (Q_{tot}(\boldsymbol{\tau}, \hat{\boldsymbol{a}}) - Q^*(\boldsymbol{\tau}, \hat{\boldsymbol{a}}))^2 + \sum_{\boldsymbol{a} \in A_r \& \boldsymbol{a} \neq \hat{\boldsymbol{a}} \& Q^*(\boldsymbol{\tau}, \boldsymbol{a}) \geq Q_{tot}(\boldsymbol{\tau}, \hat{\boldsymbol{a}})} (Q_{tot}(\boldsymbol{\tau}, \boldsymbol{a}) - Q^*(\boldsymbol{\tau}, \boldsymbol{a}))^2$$

$$+ \sum_{\boldsymbol{a} \in A_r \& \boldsymbol{a} \neq \hat{\boldsymbol{a}} \& Q^*(\boldsymbol{\tau}, \boldsymbol{a}) < Q_{tot}(\boldsymbol{\tau}, \hat{\boldsymbol{a}})} (Q_{tot}(\boldsymbol{\tau}, \boldsymbol{a}) - Q^*(\boldsymbol{\tau}, \boldsymbol{a}))^2 + \sum_{\boldsymbol{a} \notin A_r} \alpha(Q_{tot}(\boldsymbol{\tau}, \boldsymbol{a}) - Q^*(\boldsymbol{\tau}, \boldsymbol{a}))^2$$

For joint actions $\boldsymbol{a} \in A_r$ and $\boldsymbol{a} \neq \hat{\boldsymbol{a}}$ with $Q^*(\boldsymbol{\tau}, \boldsymbol{a}) < Q_{tot}(\boldsymbol{\tau}, \hat{\boldsymbol{a}})$, the loss can reach 0 ideally when $Q_{tot}(\boldsymbol{\tau}, \boldsymbol{a}) = Q^*(\boldsymbol{\tau}, \boldsymbol{a})$. But due to the monotonicity constraints of the mixing function, this idealized scenario is unlikely to occur, thus excluding this component results in a lower bound for $\mathcal{L}_{Q_{tot}}$.

When $\alpha = 0$, the loss for joint actions $\boldsymbol{a} \notin A_r$ equals zero, which also represents a lower bound for $\mathcal{L}_{Q_{tot}}$.

Therefore, we have

$$\mathcal{L}_{Q_{tot}} = (Q_{tot}(\boldsymbol{\tau}, \hat{\boldsymbol{a}}) - Q^*(\boldsymbol{\tau}, \hat{\boldsymbol{a}}))^2 + \sum_{\boldsymbol{a} \in A_r \& \boldsymbol{a} \neq \hat{\boldsymbol{a}} \& Q^*(\boldsymbol{\tau}, \boldsymbol{a}) \geq Q_{tot}(\boldsymbol{\tau}, \hat{\boldsymbol{a}})} (Q_{tot}(\boldsymbol{\tau}, \boldsymbol{a}) - Q^*(\boldsymbol{\tau}, \boldsymbol{a}))^2$$

$$+ \sum_{\boldsymbol{a} \in A_r \& \boldsymbol{a} \neq \hat{\boldsymbol{a}} \& Q^*(\boldsymbol{\tau}, \boldsymbol{a}) < Q_{tot}(\boldsymbol{\tau}, \hat{\boldsymbol{a}})} (Q_{tot}(\boldsymbol{\tau}, \boldsymbol{a}) - Q^*(\boldsymbol{\tau}, \boldsymbol{a}))^2 + \sum_{\boldsymbol{a} \notin A_r} (Q_{tot}(\boldsymbol{\tau}, \boldsymbol{a}) - Q^*(\boldsymbol{\tau}, \boldsymbol{a}))^2$$

$$\geq (Q_{tot}(\boldsymbol{\tau}, \hat{\boldsymbol{a}}) - Q^*(\boldsymbol{\tau}, \hat{\boldsymbol{a}}))^2 + \sum_{\boldsymbol{a} \in A_r \& \boldsymbol{a} \neq \hat{\boldsymbol{a}} \& Q^*(\boldsymbol{\tau}, \boldsymbol{a}) \geq Q_{tot}(\boldsymbol{\tau}, \hat{\boldsymbol{a}})} (Q_{tot}(\boldsymbol{\tau}, \boldsymbol{a}) - Q^*(\boldsymbol{\tau}, \boldsymbol{a}))^2$$

Following a similar approach, the form of $\mathcal{L}_{Q_r}$ is as follows:

$$\mathcal{L}_{Q_r} = (Q_r(\boldsymbol{\tau}, \hat{\boldsymbol{a}}) - Q^*(\boldsymbol{\tau}, \hat{\boldsymbol{a}}))^2 + \sum_{\boldsymbol{a} \in A_r \& \boldsymbol{a} \neq \hat{\boldsymbol{a}} \& Q^*(\boldsymbol{\tau}, \boldsymbol{a}) \geq Q_r(\boldsymbol{\tau}, \hat{\boldsymbol{a}})} (Q_r(\boldsymbol{\tau}, \boldsymbol{a}) - Q^*(\boldsymbol{\tau}, \boldsymbol{a}))^2$$

$$+ \sum_{\boldsymbol{a} \in A_r \& \boldsymbol{a} \neq \hat{\boldsymbol{a}} \& Q^*(\boldsymbol{\tau}, \boldsymbol{a}) < Q_r(\boldsymbol{\tau}, \hat{\boldsymbol{a}})} (Q_r(\boldsymbol{\tau}, \boldsymbol{a}) - Q^*(\boldsymbol{\tau}, \boldsymbol{a}))^2 + \sum_{\boldsymbol{a} \notin A_r} (Q_r(\boldsymbol{\tau}, \boldsymbol{a}) - Q^*(\boldsymbol{\tau}, \boldsymbol{a}))^2$$

According to Lemma 1 and Lemma 2, the losses corresponding to $\boldsymbol{a} \in A_r$ and $\boldsymbol{a} \neq \hat{\boldsymbol{a}}$ with $Q^*(\boldsymbol{\tau}, \boldsymbol{a}) < Q_r(\boldsymbol{\tau}, \hat{\boldsymbol{a}})$ as well as $\boldsymbol{a} \in A_r$ are zero.

Thus, we have

$$\mathcal{L}_{Q_r} = (Q_r(\boldsymbol{\tau}, \hat{\boldsymbol{a}}) - Q^*(\boldsymbol{\tau}, \hat{\boldsymbol{a}}))^2 + \sum_{\boldsymbol{a} \in A_r \& \boldsymbol{a} \neq \hat{\boldsymbol{a}} \& Q^*(\boldsymbol{\tau}, \boldsymbol{a}) \geq Q_r(\boldsymbol{\tau}, \hat{\boldsymbol{a}})} (Q_r(\boldsymbol{\tau}, \boldsymbol{a}) - Q^*(\boldsymbol{\tau}, \boldsymbol{a}))^2$$

$$+ \sum_{\boldsymbol{a} \in A_r \& \boldsymbol{a} \neq \hat{\boldsymbol{a}} \& Q^*(\boldsymbol{\tau}, \boldsymbol{a}) < Q_r(\boldsymbol{\tau}, \hat{\boldsymbol{a}})} (Q_r(\boldsymbol{\tau}, \boldsymbol{a}) - Q^*(\boldsymbol{\tau}, \boldsymbol{a}))^2 + \sum_{\boldsymbol{a} \notin A_r} (Q_r(\boldsymbol{\tau}, \boldsymbol{a}) - Q^*(\boldsymbol{\tau}, \boldsymbol{a}))^2$$

$$= (Q_r(\boldsymbol{\tau}, \hat{\boldsymbol{a}}) - Q^*(\boldsymbol{\tau}, \hat{\boldsymbol{a}}))^2 + \sum_{\boldsymbol{a} \in A_r \& \boldsymbol{a} \neq \hat{\boldsymbol{a}} \& Q^*(\boldsymbol{\tau}, \boldsymbol{a}) \geq Q_r(\boldsymbol{\tau}, \hat{\boldsymbol{a}})} (Q_r(\boldsymbol{\tau}, \boldsymbol{a}) - Q^*(\boldsymbol{\tau}, \boldsymbol{a}))^2$$

At this point, $\mathcal{L}_{Q_r}$ and the lower bound of $\mathcal{L}_{Q_{tot}}$ have the same form. Define $Q_r(\boldsymbol{\tau}, \hat{\boldsymbol{a}}) = m$ when $\mathcal{L}_{Q_r}$ reaches its minimum value after the full convergence of Q_r. We can construct a valid Q_{tot} that adheres to monotonicity constraints, ensuring that the minimum value of $\mathcal{L}_{Q_{tot}}$ matches that of $\mathcal{L}_{Q_r}$:

$$Q_{tot}(\boldsymbol{\tau}, \boldsymbol{a}) = \begin{cases} m + \grave{o}, \boldsymbol{a} = \hat{\boldsymbol{a}} \\ m, \boldsymbol{a} \neq \hat{\boldsymbol{a}} \end{cases}$$

Here, $\grave{o}$ is a small positive real number used to satisfy the assumption of the unique maximal joint action of Q_{tot}, without affecting the analysis of the lower bound of the loss function.

If $\hat{\boldsymbol{a}} \in A_{tgm}$, then $Q_r(\boldsymbol{\tau}, \hat{\boldsymbol{a}}) = Q_{tot}(\boldsymbol{\tau}, \hat{\boldsymbol{a}}) = Q^*(\boldsymbol{\tau}, \boldsymbol{a}^*)$, Q_{tot} has already converged with $\hat{\boldsymbol{a}} \in A_{tgm}$.

If $\hat{\boldsymbol{a}} \notin A_{tgm}$, according to Lemma 3, we know $Q^*(\boldsymbol{\tau}, \hat{\boldsymbol{a}}) < m < Q^*(\boldsymbol{\tau}, \boldsymbol{a}^*)$. Therefore, we can construct a valid Q'_{tot}

$$Q'_{tot}(\boldsymbol{\tau}, \boldsymbol{a}) = \begin{cases} Q^*(\boldsymbol{\tau}, \boldsymbol{a}^*), \boldsymbol{a} = \boldsymbol{a}^* \\ m, \boldsymbol{a} \neq \boldsymbol{a}^* \end{cases}$$

that satisfies $\mathcal{L}_{Q'_{tot}} < \mathcal{L}_{Q_{tot}}$, indicating that the current $\hat{a}$ cannot remain unchanged after Q_{tot} converges. And $\hat{a}' = \arg\max_{\boldsymbol{a}\in\boldsymbol{A}} Q'_{tot}(\boldsymbol{\tau}, \boldsymbol{a})$ satisfies $Q^*(\boldsymbol{\tau}, \hat{a}') > Q^*(\boldsymbol{\tau}, \hat{a})$.

This suggests that with the iterative training process, the value of $Q^*(\boldsymbol{\tau}, \hat{a})$ will keep rising until $\hat{a} \in \boldsymbol{A}_{tgm}$. During this period, the range of $\boldsymbol{A}_r$ will also gradually narrow down, eventually encompassing only the optimal joint actions. Thus, Theorem 2 is proven.

C Discussion

In this section, we provide a more accessible and comprehensive discussion of the motivation and design rationale underlying our work. This discussion aims to clarify the core innovations of our paper, avoiding potential misunderstandings and highlighting the novelty of our approach.

C.1 Problem Statement

The foundation of the CTDE framework is built on the IGM condition, which necessitates the use of the Q_{tot} module during training; however, due to the monotonicity constraints of the Q_{tot} mixing function, even if one agent performs the optimal action, it is still possible to receive incorrect punishment due to the suboptimal actions performed by other agents, making it difficult to accurately estimate the values of the optimal joint actions. To address this issue, WQMIX introduces an effective strategy that increases the weight of the optimal joint actions during training (Rashid et al. 2020a). This enhances the importance of accurately estimating the values of the optimal joint actions while reducing the incorrect punishment incurred from executing suboptimal joint actions.

To recognize optimal joint actions, WQMIX theoretically proposes training an unrestricted value function and exploring the entire joint action space, but since the joint action space in MARL grows exponentially with the number of agents, resulting in significant computational complexity and limiting its practicality to complex scenarios, WQMIX makes necessary approximations to derive a practical algorithm, which unfortunately introduces new approximation errors.

C.2 Design Rationale

Our purpose is to make improvement upon WQMIX by not directly searching for the optimal joint actions, but instead by recognizing a smaller set, $\boldsymbol{A}_r$, which consists of potentially optimal joint actions, and assigning higher weights to this set during training.

Specifically, our approach introduces an innovative recognition module, denoted as Q_r, where, upon convergence, each joint action value within Q_r is capable of being restored to its true value. This accurate restoration of the joint action values in Q_r ensures that A_r can be precisely identified.

To achieve this effect, when designing Q_r, we need it to satisfy three properties:

For a given state s,

a) Each joint action corresponds to an independent Q_r value. By incorporating an auxiliary variable $\boldsymbol{a}$, Q_r and Q_i break free from the monotonic relationship, ensuring that joint actions do not interfere with each other during training. This separation allows Q_r to recover the true joint action values without error.

If **a** is not an explicit input, i.e., $Q_r(\tau, \mathbf{a}) = \sum_{i=1}^{n} \lambda_i(s)(Q_i(\tau_i, a_i) - \max_{a_i \in A_i} Q_i(\tau_i, a_i)) + V(s)$, then Q_r and Q_i would have a monotonic relationship, failing to satisfy the property that different Q_r values are mutually independent.

b) Q_r satisfies IGM. Q_r still adheres to the IGM condition,i.e., $\arg\max_{\mathbf{a}\in\mathbf{A}} Q_r(s, \mathbf{a}) = \hat{\mathbf{a}}$, enabling us to find $\hat{a}$ and use $\hat{a}$ to effectively identify the entire set $\boldsymbol{A}_r$.

Q_r achieves its maximum value at $Q_r(\tau, \hat{\mathbf{a}})$, serving as a baseline for judging whether a joint action **a** is a potentially optimal joint action by comparing the values of $Q_r(\tau, \mathbf{a})$ and $Q_r(\tau, \hat{\mathbf{a}})$.

Multiplying $\lambda_i(s, \mathbf{a})$ by $(Q_i(\tau_i, a_i) - \max_{a_i \in A_i} Q_i(\tau_i, a_i))$ is a feasible way to ensure that Q_r satisfies IGM.

c) Setting Q_r Training Target as Q^*: True Joint Action Values When a joint action **a** is superior to $\hat{a}$, i.e., $Q^*(s, \mathbf{a}) > Q^*(\tau, \hat{\mathbf{a}})$, the objective for $Q_r(\tau, \mathbf{a})$ is to closely approximate $Q^*(\tau, \mathbf{a})$. Therefore, we set the training target of Q_r to mirror the true joint action values, Q^*, striving for accurate representation.

Moreover, due to the constraints imposed by the IGM condition, the Q values of all other joint actions cannot exceed that of $\hat{\mathbf{a}}$. Consequently, $Q_r(\tau, \hat{\mathbf{a}})$ serves as a "threshold" or "boundary." If the Q value of another joint action is below this threshold, its corresponding Q_r is learned to reflect its true value; if it exceeds this threshold, its Q_r is constrained by the IGM condition to $Q_r(\tau, \hat{\mathbf{a}})$.

With the above three properties, we can define potentially optimal joint actions using Q_r. Taking $Q_r(\tau, \hat{\mathbf{a}})$ as the baseline, if there are joint actions that may be optimal, then due to the independence between Q_r values, and Q_r being as high as possible while satisfying IGM, when $Q_r(\tau, \mathbf{a}) = Q_r(\tau, \hat{\mathbf{a}})$, $\mathbf{a}$ is a potentially optimal joint action. This is also the origin of Definition 1.
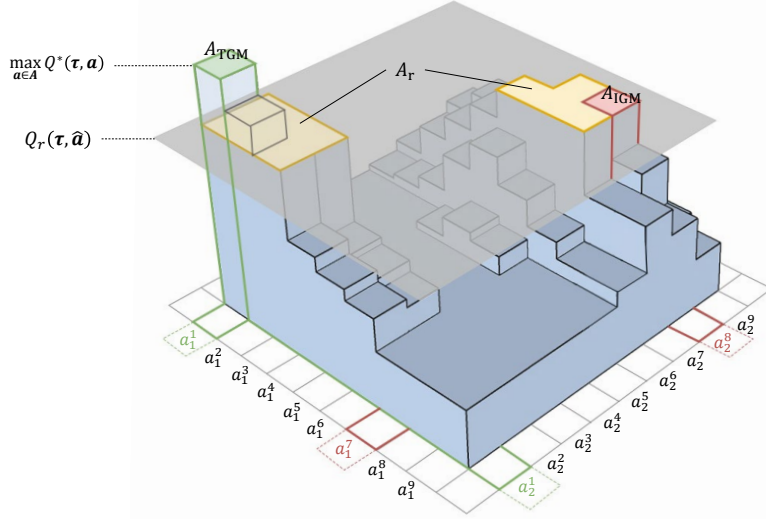

Figure 7: This figure illustrates the Q-value landscape, where the height of each column represents the Q-value associated with a particular joint action. The exact heights are not critical for the concepts discussed herein. The current convergence state of the Q_r network resembles Stage 2 in Figure 8. The red area represents $\hat{\mathbf{a}}$. The yellow area highlights A_r, which is determined via $\hat{\mathbf{a}}$ and represents the subset of actions on which POWQMIX focuses its weighted training efforts. The green area denotes the global optimal joint actions. For Q_r, the Q-values beneath the conceptual plane are already learned, while the Q-values within A_r are set at the plane's level. As the training progresses, the plane is expected to rise incrementally, identifying increasingly higher Q-values.

As Q_r and Q_{tot} iterate, the $\boldsymbol{A}_r$ set will gradually converge to the optimal joint actions, and Q_r will learn the true joint action values, enabling our new weighting method to ultimately let Q_{tot} recover the optimal policy.

Note: The assumption regarding the uniqueness of optimal joint action seems strong, but in practical applications, it is acceptable. Because the values of $Q_i(\tau, a)$ are computed by the network, and these values are influenced by various factors such as historical observations, reward functions, data distribution, etc., it is unlikely for different actions to have the same $Q_i(\tau, a)$, at least within the context and experiments discussed in this paper. Therefore, $\hat{a}$ and optimal joint action is typically unique.

C.3   Illustrative Example

Figure 8 is an example illustrating how POWQMIX overcomes non-monotonicity issues.

We take the matrix game in the paper as an example for better presentation of the theory of POWQMIX.

The action space is A, B, C. In this kind of one-step matrix game, Q^* and $\hat{Q}^*$ are exactly equivalent to the true reward function. In the training process, POWQMIX will roughly go through three stages I, II and III.

In the I and II stages, based on the values of Q_r, we can infer that only the joint actions (A,A) and (C,C) are potentially optimal joint actions, with weights equal to 1, while the weights for all other joint actions are 0. In the II stage, the Q_{tot} corresponding to the joint action (C,C) is the same as Q^*, so the training gradient is 0. However, for the joint action (A,A), $Q_{tot} < Q^*$, so after training, the Q_{tot} corresponding to joint action (A,A), as well as $Q_1(\tau_1, A)$ and $Q_2(\tau_2, A)$, will all increase until the III stage. At this point, only (A,A) remains a potentially optimal joint action, consistent with the true optimal joint action, and the algorithm successfully escapes from the local optimum of 7.9 and converges to the global optimum.

Here we highlight the differences with QPLEX, in QPLEX, all joint action weights are set to 1 during training, making it unable to escape the local optimum of 7.9. Furthermore, due to the instability of QPLEX, it is difficult to converge in this matrix setting, leading to significant errors in joint action value evaluation. This phenomenon can be observed in the experimental results in both POWQMIX and ResQ papers.

Figure 8: Three stages of the matrix game. The potentially optimal joint action is highlighted with a yellow border.

D Experimental Setup

D.1 Implementation Details and Hyperparameters

We run all experiments based on the PyMARL2 framework. Some important hyperparameters are listed in Table 2. If not specified, the default weights for potentially optimal joint actions and other joint actions in POWQMIX are 5 and 0. The constant C used in Equation 11 is set to 0.05. The weights for optimal joint actions and other joint actions in CW-QMIX and OW-QMIX are 1 and 0.1.

hyperparameter	value
optimizer	Adam
batch size(episodes)	128
replay buffer size(episodes)	5000
rollout processes	8
ϵ start	1
ϵ finish	0.05
ϵ anneal steps	500k
$TD(\lambda)$	0.6

Table 2: Hyperparameters

D.2 Matrix Game

We set $\epsilon = 1$ throughout the experiments on matrix game to achieve uniform data distribution and set ideal weights for the purpose of theoretical analysis. The weights for potentially optimal joint actions and other joint actions in POWQMIX are 1 and 0. The weights for optimal joint actions and other joint actions in CW-QMIX and OW-QMIX are 1 and 0.

D.3 Predator-Prey

The default experimental settings are consistent with those in the PyMARL2 framework. We Specifically set ϵ anneal steps to 1500k to enhance exploration when mis-capture punishment is -3, and 4500k when mis-capture punishment is -4 and -5.

D.4 SMAC

In the PyMARL2 framework, certain parameters such as hidden size and $TD(\lambda)$ have been specifically fine-tuned for the 6h_vs_8z and 3s5z_vs_3s6z maps. However, for the sake of a fair comparison, we set all algorithms to use default parameters across all maps.